ELSEVIER

Polymer 44 (2003) 1941–1947

polymer

www.elsevier.com/locate/polymer

A molar mass induced transition in the yielding properties of linear polyethylene

Q. Fu, Y. Men, G. Strobl*

Fakultät für Physik, Albert-Ludwigs-Universität, Hermann-Herder-Str. 3, 79104 Freiburg, Germany

Abstract

The mechanism of tensile deformation in a semi-crystalline polymer like PE changes at four critical points which can be associated with (A) the onset of single slip-processes, (B) a turnover into a collective activity of slips, (C) the beginning of a disaggregation of the crystal blocks, followed by fibril formation, and (D) the onset of chain disentangling. Studies of the deformation behavior of series of LPEs with increasing molar mass show an abrupt rise of the critical strains ε_H(C) and ε_H(D) at a molar mass of $M_t \approx (1\ 5-2) \times 10^5$ g mol^{-1}. As indicated by dynamic mechanical tests the rise originates from a change in the mobility and compliance of the amorphous regions, which are melt-like for $M_w > M_t$, but reduced for $M_w < M_t$. As a consequence, both, crystal block disaggregation and chain disentangling, set in at lower strains.

Keywords: Polyethylene; Deformation

1. Introduction

An investigation of the tensile deformation behavior of various polyethylenes, linear, short-chain branched as well as copolymerized samples, covering a crystallinity range from 70 to 10% showed us that they all follow a common scheme with remarkable invariances [1,2]. The scheme becomes apparent in the true stress-strain curves at constant strain rate, obtained with the aid of a video-controlled tensile testing machine, and in step-cycle measurements of the elastic recovery. The results demonstrate the existence of four critical points, where the differential compliance, the recovery properties and the evolution of the crystalline texture change simultaneously. They are associated with qualitative changes of the deformation mechanism, as we understand it, with

1. the onset of isolated inter-and intralamellar slip processes (point A),
2. a turnover into a collective activity of slips (B),
3. the beginning of crystallite fragmentation and fibril formation (C),
4. the onset of chain disentanglement (D).

As a most interesting characteristic result it was found that while the stresses at the critical points increased together with the crystallinity, the strains at these points remained practically constant. The same invariance of the critical strains holds also when the temperature or, within the possible range, the strain rate is changed. The invariance of the critical strains, i.e. the strain control of the deformation behavior, implies that the strain can be considered as homogeneous in semi-crystalline polymers. We may conclude that the crystallites in the sample can easily react on, i.e. take up the imposed strain. This looks difficult if one would have to deal with stiff, laterally extended, stacked lamellae. Indeed, evidence is growing that the lamellae generally possess a blocky substructure [3–5]. The then possible intralamellar block-slips, together with the two independent modes of interlamellar shear, offer sufficient degrees of freedom to achieve it.

Generally, the applied load is transmitted by both, the skeleton set up by the crystallites and the entanglement network of the amorphous regions. During a deformation process, the respective weights change. At low deformations, load is first of all transmitted by the crystals, at high deformations the network forces become dominant. Correspondingly, the yield point (B) is a property of the crystalline skeleton, which above B experiences a continuous readjustment by block-slips. Point C marks the end of the stability of the blocks. From there on and continuing

* Corresponding author. Tel.: +49-761-203-5887; fax: +49-761-203-5855.
E-mail address: strobl@uni-freiburg.de (G. Strobl).

0032-3861/03/$ - see front matter © 2003 Elsevier Science Ltd. All rights reserved.
doi:10.1016/S0032-3861(03)00036-3

further on, they become destroyed under the action of the network forces, and fibrils form which again possess an internal block structure. Finally, at large deformations, behavior is dominated by the forces produced by the stretched entanglement network. One observes a rubber-like curve independent of the crystallinity or the temperature.

Bayer carried out tensile tests on a series of linear polyethylenes under variation of the molar mass in the range from $(0.5-3)\times 10^5$ g mol^{-1} and observed in his experiments an abrupt change in the deformation properties around $M_t \approx 1.5\times 10^5$ g mol^{-1}, a value far above the critical molar mass M_c associated with the onset of entanglement effects [6]. There, he observed a pronounced increase in the samples elasticity showing up in the strain recovery, accompanied by other changes like an increase in the degree of orientation on injection moulding. Bayer concluded that this change must be due to a modification of the properties of the entanglement network rather than a change in the properties of the crystallites. He furthermore offered a tentative explanation, proposing that rather than being homogeneous the distribution of entanglements in a polymer melt may include entanglement concentrations which he calls 'knots'. Bayer argues that knot formation sets in just at this molar mass M_t [7].

When we learned about Bayer's work we checked our data, finding out that all LPE samples we had investigated had molar masses above M_t. We now extended our investigations to the range of lower molar masses and measured again the critical strains at A, B, C and D. The results are reported in the following. They are clear and fully confirm the observations of Bayer. We find abrupt changes of the critical strains at C and D. Opposite to it there is no effect on point A and the yield point B. The results are again based on measured true stress–strain curves and are therefore quite reliable. To learn about the possible origin of the effect we combined the tensile tests with small angle X-ray scattering for a structure determination, and dynamic mechanical measurements for probing the mobility in the amorphous phase. The results indicate that the transition in the yielding properties originates from a mobility change in the amorphous intercrystalline layers.

2. Experimental section

2.1. Samples

Experiments were conducted on a variety of commercial linear polyethylenes (LPEs) with molar masses in the range $M_w = (0.67-36)\times 10^5$ g mol^{-1}. They are specified with their trade names in Table 1. Dog-bone samples appropriate for the mechanical tests were cut out of films with a thickness of 0.5 mm which were crystallized by a slow cooling from the melt. Crystallinities as deduced from the heat of fusion measured in a DSC varied between 0.79 for the lowest molar masses and 0.52 for the highest molar masses. We also prepared blends of the samples PE8 and PE26, by mixing them in a melt extruder.

Table 1
Linear polyethylenes used for the study

Trade name	M_η ($\times 10^5$)	M_w ($\times 10^5$)	M_w/M_n (–)	Crystallinity (ϕ_w)
PE5	0.5	0.67	7.5	0.66
PE8	1.0	1.34	7.5	0.75
PE9	5.6	7.5	7.5	0.62
PE11	1.7	2.3	7.5	0.68
PE12	11	14.7	7.5	0.64
PE18	27	36	7.5	0.52
PE26	4.1	5.5	7.5	0.67
PE27	2.9	3.9	7.5	0.76
Vestolen A6016	0.52	0.58	8.17	0.79
Vestolen A6014	0.75	0.71	6.45	0.70
Vestolen A6013	0.88	0.8	6.61	0.75
Lupolen 6021D	1.61	1.83	7.22	0.73
Lupolen 5261Z	2.48	4.78	12.22	0.70

2.2. Mechanical stretching tests

All the investigated samples showed a necking on stretching. True stress-strain curves were measured with an INSTRON 4301 machine, equipped with a homebuilt video-control which regulated the crosshead speed so that a constant strain rate was maintained in the narrowed part of the specimen. In the construction of the device we followed an idea first brought up by G'Sell [8]. Recovery properties of the samples at various deformations were deduced from the amount of free shrinkage after an opening of one of the clamps. We determined also in this case the increase in the neck diameter, which relates—under the obvious assumption of an invariant volume—to the change in strain. The observation of the amount of free shrinkage enables the total Hencky-strain ε_H to be split up in the shrunk part $\varepsilon_{H,s}$ representing the elastic contribution, and the remaining part $\varepsilon_{H,r}$, representing the plastic contribution:

$$\varepsilon_H = \varepsilon_{H,r} + \varepsilon_{H,s}$$

For each determination of the amount of free shrinkage after a deformation to some strain ε_H we used a new sample.

More experimental details were given previously [1].

2.3. Dynamic mechanical measurements

The linear visoelastic properties of the samples were obtained by measurements of the complex elastic modulus using the Solid Analyzer II of Rheometrix. Characterization was based on temperature-dependent measurements at a fixed frequency of 1 Hz.

2.4. Small angle X-ray scattering

To characterize the crystalline-amorphous morphology

small angle X-ray scattering (SAXS) experiments were carried out. We used a conventional Cu K_α X-ray tube and a Kratky-compact camera together with a position-sensitive detector. After applying a desmearing procedure to obtain the pinhole scattering curve, we derived from it the interface distance distribution function by a Fourier transformation. It directly shows the thickness of the amorphous layers d_a. Details about the procedure have been repeatedly given, for example in Ref. [9] or [10].

3. Results

3.1. Drawing behavior

Fig. 1 shows the change in the true stress σ with the true (Hencky-)strain ε_H, as obtained in video-controlled stretching experiments for four samples with molar masses between 0.67×10^5 and 14.5×10^5 g mol^{-1}. All the tests were carried out at room temperature with a strain rate of 5×10^{-3} s^{-1}. As can be seen directly, the strain at the yield point (B), here given as the point with the maximum curvature, is constantly around $\varepsilon_H \simeq 0.1$. The associated yield stress which is generally related to the crystallinity does not vary between the samples PE5, PE26 and PE12, which all have the same crystallinity, $\phi_c = 0.66 \pm 0.02$, and is somewhat higher for PE8 with $\phi_c = 0.75$. On the other hand, differences show up in the strain hardening at higher deformation, which becomes more intense with increasing molar mass.

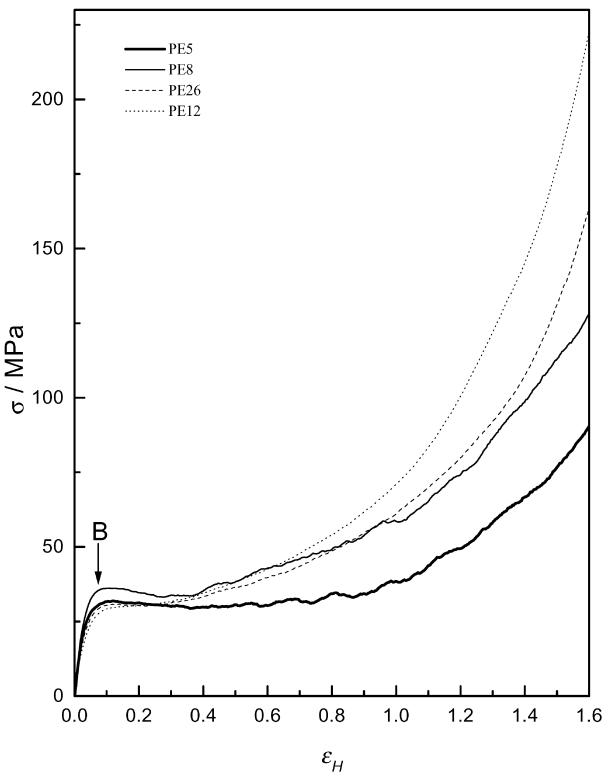

Fig. 1. Four LPEs out of the series of samples in Table 1: true stress–strain curves measured in video-controlled drawing tests at room temperature for a strain rate of 5×10^{-3} s^{-1}.

The best method to determine point C, which marks the onset of fibril formation, is in our experience the determination of the amount of free shrinkage in dependence of the total strain. Fig. 2 shows the results obtained for two samples, at room temperature and two higher temperatures. The quantity given as a function of ε_H is the plastic part of the deformation, $\varepsilon_{H,r}$, which remains after the complete unloading and a waiting time of 10 min. All curves show two critical points, the one denoted A,B marking the onset of plastic flow, i.e. the yield point (for this low resolution the end of the Hookean ideally-elastic range (A) and the yield point (B) are not separated from each other), and in addition point C, indicated by an abrupt change in the slope of the curve. As can be noted, although the yield point is the same for both samples there is a clear change in the critical strain C. For the sample with the lower molar mass we find $\varepsilon_H(C) = 0.4$ while for the sample with the higher molar mass it is found at the location $\varepsilon_H(C) = 0.6$ known from the previous studies. As in all previous studies, temperature is seen to affect the critical stresses but not the values of the strains.

The values $\varepsilon_H(C)$ of the critical strains at the onset of fibrillation obtained by free shrinkage tests for the whole series of samples are shown in Fig. 3. The curve $\varepsilon_H(C)$ as a function of M_w is well-defined. There is a region with lower values for low molar masses and a range with much higher values for the high molar masses. The change between two ranges takes place at molar masses of $M_t(1.5–2) \times 10^5$ g mol^{-1}. The results imply that the destruction and transformation of the original lamellae into fibrils occurs much earlier for the low molar masses.

It is a second peculiar property of the critical point C that the elasticity, as expressed by the amount of shrinkage $\varepsilon_{H,s}$, here reaches its maximum value. In the case of sample PE8 this maximum elastic strain amounts to

$$\varepsilon_{H,s} = \varepsilon_H - \varepsilon_{H,r} = 0.4 - 0.2 = 0.2$$

at room temperature and $\varepsilon_{H,s} = 0.3$ at 85 °C. The corresponding values for sample PE27 are $\varepsilon_{H,s} = 0.25$ and 0.4 (at 70 °C). Hence, the sample with the higher molar mass has the higher elasticity, which confirms Bayer's observations.

Whether or not as a result of a stretching a disentangling of the chains takes place can again be checked by free shrinkage experiments, when they are accompanied by a heating to temperatures near to the melting point. As long as there is no disentangling, the heating will bring the sample back to its original length. The retraction is due to the entanglement network and it can only be complete if the original network remains unchanged. Disentangling processes change the network and therefore result in an incomplete retraction. The criterion can be used to determine point D where disentangling sets in, and Fig. 4 shows the results thus obtained for the series of samples. Again one observes

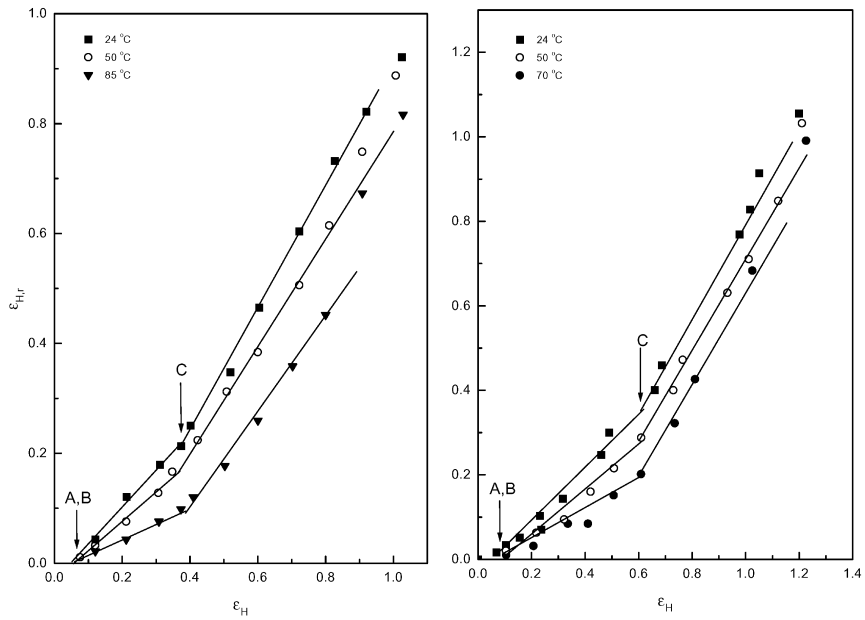

Fig. 2. Samples PE8 (left) and PE27 (right): strain $\varepsilon_{H,r}$ remaining after the free shrinkage subsequent to a video-controlled stretching to various values ε_H. Drawing was carried out at three different temperatures. Experiments give the location of the critical strain $\varepsilon_H(C)$ at the onset of fibrillation.

an abrupt change in the molar mass range $M_t = (1.5–2) \times 10^5$ g mol^{-1}. For the low molar mass part, the critical strain $\varepsilon_H(D)$ is shortly above the critical strain $\varepsilon_H(C)$, for higher molar masses the two points are well separated. For molar masses $M_w > 10^6$ g mol^{-1} no disentangling took place up to the point of fracture. Interesting to note, a tentative continuation of the line in the low molar mass parts down to $\varepsilon_H(D) = 0$ leads to a molar mass near to the value Mc where entanglement effects are for the first time found in the viscoelastic properties of a polyethylene melt.

Asking about the origin of this behavior we investigated the linear viscoelastic properties of the samples and carried out a structure determination by SAXS.

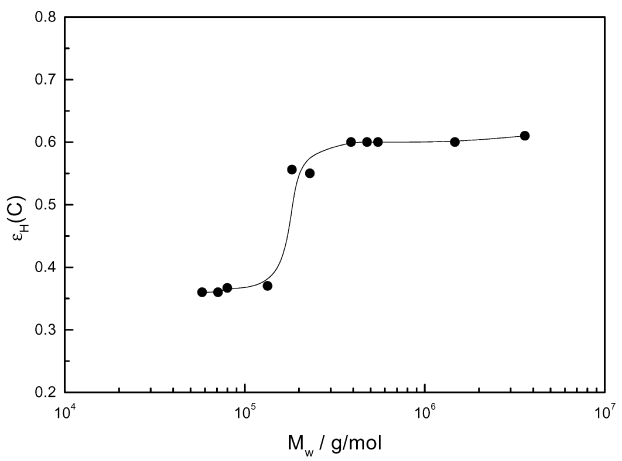

Fig. 3. Series of LPEs from Table 1: critical strains $\varepsilon_H(C)$ in dependence on the molar mass.

3.2. Dynamic mechanical tests

Fig. 5 shows the results of a temperature dependent dynamic mechanical analysis (DMA) carried out for five of the samples. Temperature runs were started immediately after a cooling from ambient temperature to − 60 °C. Curves show the real part of Young's modulus, E' and the loss tangent tan δ as obtained for a fixed frequency of 1 Hz. A clear difference in the deformation properties shows up between the samples belonging to the low molar mass group and the high molar mass group. For $M_w < M_t = 1.5 \times 10^5$ g mol^{-1} the β-process is absent; there is neither a step in $E'(T)$ nor a peak in tan $\delta(t)$. For samples with molar masses $M_w > M_t$ the β-process clearly shows up. Hence, for the latter samples a glass transition takes place in the

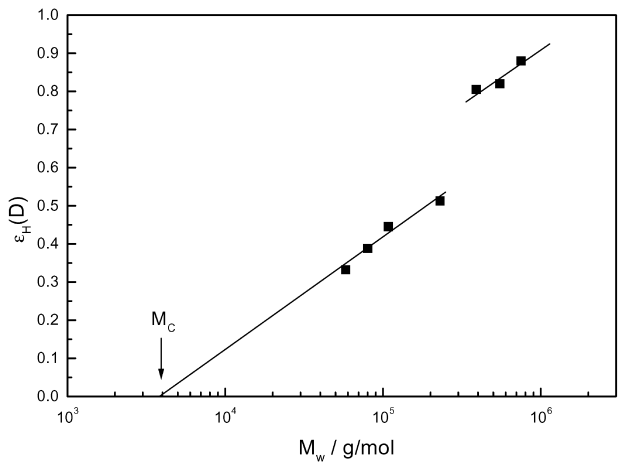

Fig. 4. Series of LPEs from Table 1: critical strains $\varepsilon_H(D)$ at the onset of disentangling processes in dependence on the molar mass. M_c is the molar mass at the entanglement limit of PE-melts.

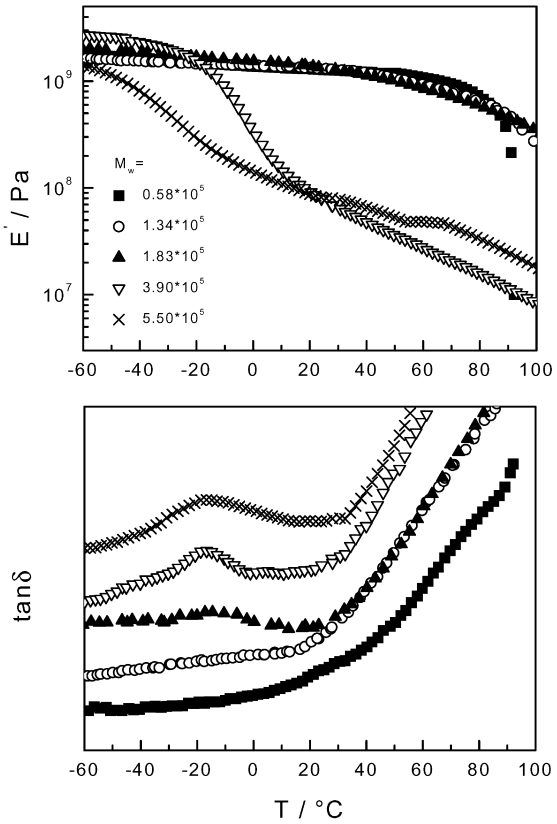

Fig. 5. Five LPEs out of the series of samples in Table 1: temperature dependence of E' and tan δ measured at a frequency of 1 Hz.

amorphous regions, whereas for the samples with molar masses below M_t the mobility in the amorphous layers is so much reduced that it is no longer melt-like. The sample with $M_w = 1.83 \times 10^5$ g mol^{-1} is just in the crossover range.

Similar observations during dynamic mechanical tests on a series of LPEs with various molar masses were recently reported by Nitta et al. [11].

3.3. Characterization by SAXS

Fig. 6 shows as an example for one of the samples the SAXS curve together with the derived one-dimensional electron density autocorrelation function $K(z)$. The peak in the scattering curve indicates a long spacing of $L = 1/0.037$ nm$^{-1} = 27$ nm. For crystallinities above 50% the self-correlation triangle in $K(z)$ relates to the amorphous layers. The mean value of their thickness, following from a continuation of the linear part down to the base line, is 5 nm. Fig. 7 shows all amorphous layer thicknesses thus obtained, given as function of the molar mass. Beginning at the limiting value of about 5 nm there is not much change for the molar masses below M_t. Then, however, for molar masses above M_t the amorphous layer thickness steadily increases. A similar result can be found in one of Bayer's papers [7].

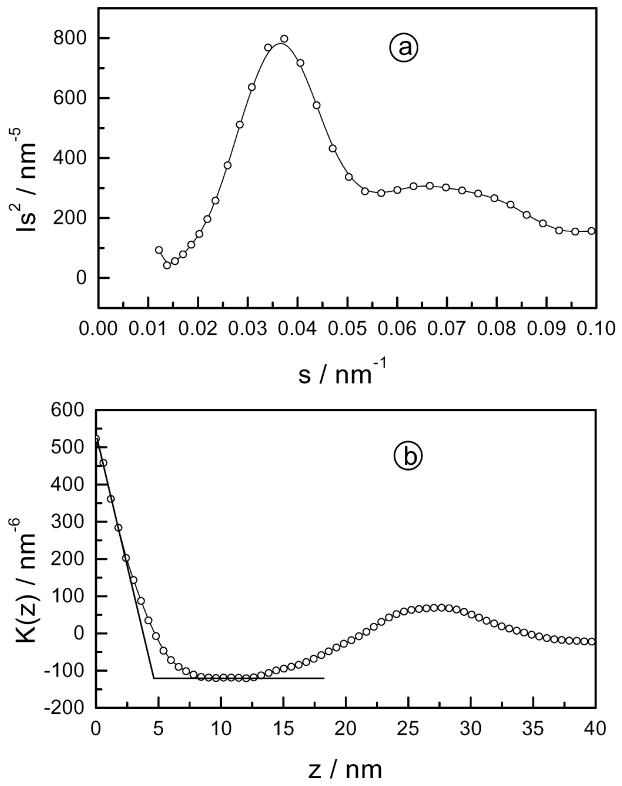

Fig. 6. Vestolen A6016: SAXS-curve (a) and deduced electron density correlation function (b). The self-correlation triangle at the origin is associated with the amorphous layers.

3.4. Results for binary mixtures

In order to complement the experiments we carried out analogous investigations for binary blends pre-pared from PE8 and PE26; P8 belongs to the low molar mass and P26 to the high molar mass group. Crystallization did not lead to a separation of the two components; the homogeneity of the mixture is obviously retained. This is indicated by Fig. 8, showing for a series of blends a continuous shift of the long

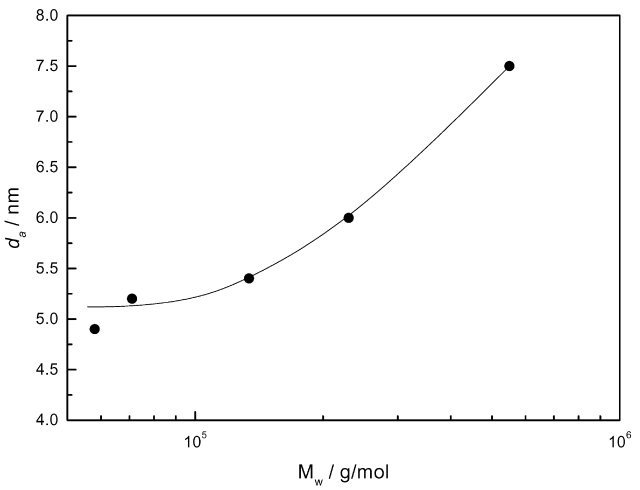

Fig. 7. Variation of the average thickness d_a of the amorphous layers with the molar mass as derived from the electron density correlation functions.

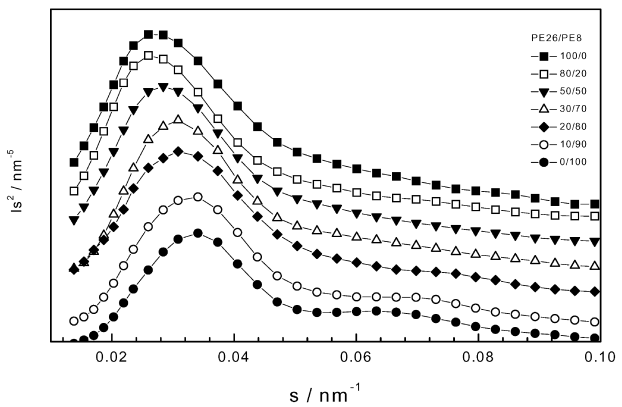

Fig. 8. Blends of different composition prepared from PE8 and PE26: SAXS curves showing a continuous shift of the long spacing peak.

spacing with the composition. We determined the critical strains $\varepsilon_H(C)$ of the blends again by free shrinkage tests. The results are shown in Fig. 9. Here, the observed critical strains are plotted as a function of the weight average molar mass

$$M_w = \phi M_1 + (1 - \phi)M_2,$$

$$M_1 = 1.34 \times 10^5, \quad M_2 = 3.9 \times 10^5 \text{ g mol}^{-1}$$

When represented as a function of the composition, the blends show a smooth transition from the low value associated with PE8 to the higher value of PE27. The continuous line in the plot is that of Fig. 3. It describes the dependence quite well.

4. Discussion

Semi-crystalline polymers are multi-phase systems where a skeleton of crystallites with rigid-amorphous surface layers is embedded in-and coupled to-a fluid entanglement network. The deformation behavior reflects properties of both components, with a dominance of the

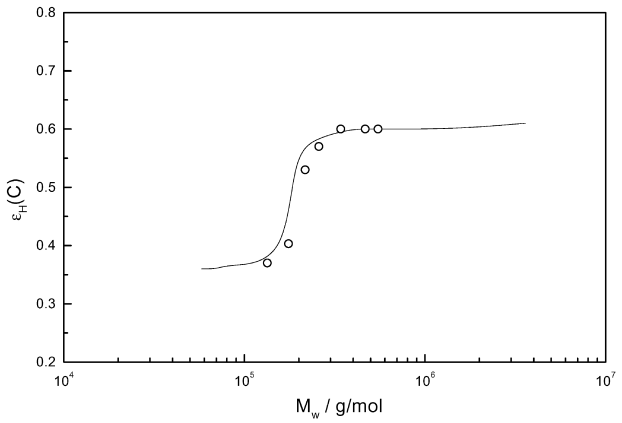

Fig. 9. Blends of different composition prepared from PE8 and PE26: critical strains $\varepsilon_H(C)$ in dependence on the weight averaged molar mass. The continuous line is taken from Fig.3.

crystalline parts in the initial stages up to the yield point B, and a major influence of the entanglement network after the destruction of the original crystal blocks beginning at point C. As we observe effects of the molar mass on the location of the critical points C and D, and not on A and B, it is obvious that we deal here with a change in the properties of the entanglement network. This is indeed confirmed by the DMA results, and they provide, together with the structural data deduced from the SAXS experiment, an explanation of the effects.

If a polymer melt crystallizes, entanglements are shifted into the amorphous regions, rather than being resolved, which is not possible with the limited time given. As a consequence, the topology and mobility of the chain sequences in the amorphous regions of semi-crystalline polymers differ from the melt. In particular, for polymers with a high degree of crystallinity like LPE, the increase in the entanglement density results in a reduction in the mobility, and a further reduction follows from the fixing of the chains in the crystallites. According to the DMA observations, this occurs here for the class of materials with molar masses below M_t. The influence of the molar mass on the mobility is thereby due to two factors. First, as shown by the data in Table 1, the low molar mass compounds have in tendency the higher crystallinity, hence, in the amorphous regions a higher entanglement density. Second, as shown by the SAXS results, they have thinner amorphous layers, with $d_a \approx 5$ nm. The thinner the layer, the larger the fraction of chain sequences immobilized by the adjacency to the crystal surface. As it appears, a surface layer with a thickness of about 2.5 nm is generally immobilized, i.e. forms a 'rigid amorphous' phase which does not show the (β-)glass transition. Liquid–amorphous parts therefore only exist in amorphous layers with thicknesses above 5 nm, where they are found in the central region away from the crystal surfaces.

The cause of the increase in d_a with M_w is the increase in the distance L between neighboring crystal lamellae. As pointed out by Rault [12], L scales with the radius of gyration R_g according to

$$L \sim R_g \sim M^{1/2}$$

When, on the other hand, the crystal thickness is constant (compare, for example the PEEK results of Dosière et al. [13]) the amorphous layer thickness increases with M_w.

Having a higher entanglement density and a larger fraction of chain sequences with one end fixed in the crystals, the amorphous layers in the low molar mass class of LPEs develop at a given shear deformation a higher shear stress. As a result, the critical stress leading to a destruction of crystal blocks and the critical stress required for a disentangling are reached earlier during the deformation, and this is our observation. The shift of $\varepsilon_H(C)$ from 0.6 for the samples of the high molar mass group to 0.4 for the lower molar mass group and the abrupt increase of $\varepsilon_H(D)$ at

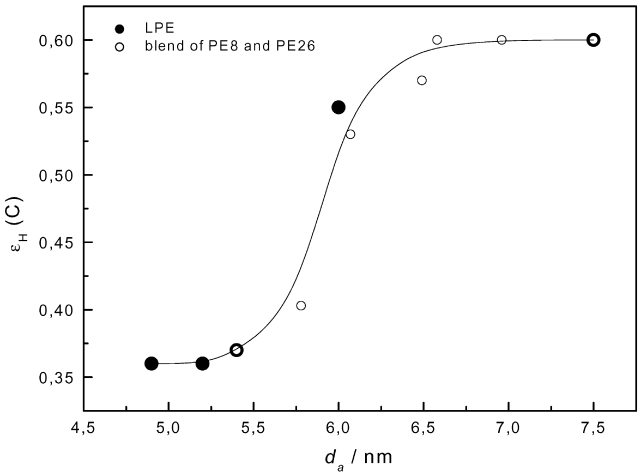

Fig. 10. Pure samples of different molar mass and blends: critical strains $\varepsilon_H(C)$ represented as a function of the amorphous layer thickness d_a.

M_t thus can be understood as reflecting a change in the shear modulus of the entanglement network, to higher values for the low molar mass group.

In the title of this contribution, we refer to the observed effect of the molar mass on the deformation properties, however, this relation is only an indirect one. The direct relationship is that to the shear modulus of the amorphous regions, which changes, first of all, with their thickness d_a. To show this physical background, it is better to represent $\varepsilon_H(C)$ as a function of d_a, rather than M_w. This is carried out in Fig. 10 which includes both, the data for the blends and the individual components. That d_a and not M_w is the appropriate parameter for describing the effects becomes also clear, when we include PEs with short chain branches or co-units into the considerations. All these compounds show the glass-(β-) transition, independent of the molar mass, because the crystallinity is lower and the amorphous layers are correspondingly thicker. Indeed, we found for all these compounds in fact the normal, higher value of the critical strain, $\varepsilon_H(C) = 0.6$, and some of the investigated compounds had molar masses even below that of PE5 [1].

To conclude, the deformation properties of a semi-crystalline polymer can be affected either by changing the coupling between the crystal blocks setting up the crystal skeleton, or by changing the elastic properties of the entangled amorphous layers. We give here an example for the second case and use the molar mass to induce the changes.

Acknowledgements

This work would not have been carried out without the continuous support by Rüdiger Bayer (Gesamt-Hochschule Kassel). He initiated it with a seminar talk in our group, provided us with additional samples and helped us with steady advice. Funding of this work came from the Deutsche Forschungsgemeinschaft (Sonderforschungsbereich 428) and is gratefully acknowledged. Thanks are also due to the ‘Fonds der Chemischen Industrie’ for financial help.

References

[1] Hiss R, Hobeika S, Lynn C, Strobl G. Macromolecules 1999;32:4390.
[2] Hobeika S, Men Y, Strobl G. Macromolecules 2000;33:1827.
[3] Loos J, Thüne PC, Lemstra PJ, Niemantsverdriet JW. Macromolecules 1999;32:8910.
[4] Magonov S, Godovsky Y. Am Lab 1999;31.
[5] Hugel T, Strobl G, Thomann R. Acta Polym 1999;50:214.
[6] Bayer RK, Liebentraut F, Meyer T. Colloid Polym Sci 1992;270:331.
[7] Bayer RK. Colloid Polym Sci 1994;272:910.
[8] G’Sell C, Hiver JM, Dahoun A, Souahi A. J Mater Sci 1992;27:5031.
[9] Albrecht T, Strobl GR. Macromolecules 1996;29:783.
[10] Schmidtke J, Strobl G, Thurn-Albrecht T. Macromolecules 1997;30:5804.
[11] Nitta K, Tanaka A. Polymer 2001;42:1219.
[12] Robelin-Souffache E, Rault J. Macromolecules 1989;22:3582.
[13] Fougnies C, Dosiére M, Koch MHJ, Roovers J. Macromolecules 1998;18:6266.